Cell Stress and Chaperones (2020) 25:793–802
https://doi.org/10.1007/s12192-020-01133-w

ORIGINAL PAPER

RUNX3-dependent oxidative epithelial-to-mesenchymal transition in methamphetamine-induced chronic lung injury

Lin Shi[1] · Bing-Yang Liu[2] · Xin Wang[1] · Mei-Jia Zhu[1] · Lei Chen[1] · Ming-Yuan Zhou[1] · Ying-Jian Gu[1] · Lin Cheng[1] · Yun Wang[1]

Received: 18 April 2020 / Revised: 22 June 2020 / Accepted: 25 June 2020 / Published online: 17 July 2020

Abstract

Lung toxicity is the main cause of the death from methamphetamine (MA) abuse, but its mechanism has remained unclear. The purpose of our study was to investigate if MA can induce epithelial-to-mesenchymal transition (EMT) and if RUNX3 is involved in oxidative EMT in MA-induced chronic lung injury. The rats were divided into the control group and MA group. Extracted lungs were used for morphological measurements and Western blot. The alveolar epithelial cells were cultured or transfected and then treated with MA or/and N-acetyl cysteine (NAC) followed by flow cytometry, Western blot, and immunohistochemistry. Chronic exposure to MA resulted in the lower growth ratio of weight, increased right ventricular index, thickened alveolar walls, and reduced number of alveolar sacs. Long-term administration with MA caused oxidative stress and pulmonary EMT. NAC increased RUNX3 and alleviated EMT. However, after knockdown of RUNX3, reactive oxygen species (ROS) levels were significantly upregulated, indicating that RUNX3 was closely related to oxidative stress. Knockdown of RUNX3 aggravated MA-induced EMT by activating RUNX3-dependent TGF-β signaling. Therefore, RUNX3 may be the key to oxidative EMT in methamphetamine-induced chronic lung injury.

Keywords RUNX3 · Epithelial-to-mesenchymal transition · Oxidative · Methamphetamine · Lung · TGF-β

Introduction

The abuse of methamphetamine (MA) is a major public health issue (Wang et al. 2018). MA is an addictive drug with popularity among the young and the middle-aged adults (Orcholski et al. 2017). A study has found that when injecting MA in humans, 24–31% of the dose is absorbed by lung (Volkow et al. 2010). A higher uptake rate of MA in lungs resulted in toxicity and some lung diseases such as pulmonary hypertension and pulmonary edema (Albertson et al. 1999; Ciccarone 2011; Ramirez et al. 2018). Pulmonary dysfunction is the main cause of the death from MA toxicity, but its mechanism has remained unclear.

Runt gene family members (RUNX1, RUNX2, and RUNX3) play the important roles in the normal development of tissues and carcinogenesis. RUNX1 was first recognized as a tumor suppressor in myeloid leukemia. RUNX1 is indispensable for the hematopoietic system and is one of the most commonly mutated genes in a variety of hematological malignancies (Link et al. 2010; Sood et al. 2017). RUNX2 is essential for skeletal development and osteoblast differentiation (Komori 2017). RUNX3, as a tumor suppressor, not only is involved in the tumor formation but also plays a key role in cellular growth, embryonic development, and immune regulation (Ito et al. 2015; Lotem et al. 2015). Although a large number of studies on RUNX3 are focused on cancer metastasis, RUNX3 is also an important regulator of pulmonary angiogenesis and plays a vital role in lung development (Lee et al. 2014). Mice with loss of RUNX3 can show the abnormal alveolar dysplasia 1 day after birth (Lee et al. 2010). Since RUNX3 is expressed in lungs and takes part in the lung development, we wondered whether RUNX3 is also involved in the mechanism of chronic lung injury induced by MA.

Lin Shi and Bing-Yang Liu contributed equally to this work.

✉ Yun Wang
ywang28@cmu.edu.cn

[1] Department of Clinical Pharmacology, School of Pharmacy, China Medical University, No.77 Puhe Road, Shenyang North New Area, Shenyang 110122, Liaoning, People's Republic of China

[2] Department of Endocrinology, Shengjing Hospital of China Medical University, Shenyang 110004, Liaoning, People's Republic of China

Our previous study found that MA increased the ROS levels and the accumulation of ROS which resulted in oxidative stress in rat lungs (Franco et al. 2008; Bai et al. 2017), indicating that oxidative stress participated in the MA-induced lung toxicity (Wang et al. 2018). Oxidative stress inhibited activation of RUNX3 in human colon cancer cells (Kang et al. 2013). This suggested to us that RUNX3-related oxidative stress is probably associated with MA-induced chronic lung injury.

Chronic lung injury clinically includes chronic inflammation, pulmonary hypertension, chronic obstructive pulmonary disease (COPD), pulmonary fibrosis, and even lung cancer. Among these chronic lung diseases, epithelial-to-mesenchymal transition (EMT) is a vital pathology (Stone et al. 2016). EMT has been divided into three types: the first is to promote organ development; the second is related to organ regeneration and fibrosis; and the third is closely related to cancer infiltration and metastasis (Choi and Diehl 2009). EMT can make alveolar epithelial cells obtain mesenchymal cell phenotype, so that the deposition of extracellular matrix further promotes the pulmonary remodeling (Stone et al. 2016; Jolly et al. 2018). Therefore, EMT is also likely to be the key to the pathogenesis of MA-induced chronic lung injury. In some studies on the cancer, low levels of RUNX3 can induce EMT (Whittle and Hingorani 2015; Chen et al. 2017; Kulkarni et al. 2018). Taken together with the above, RUNX3 may play an important role in EMT induced by chronic exposure to MA.

Based on the above, the purpose of our present study was to investigate if long-term exposure to MA can induce EMT, if RUNX3 is related to oxidative stress and EMT formation, and how RUNX3-related oxidative stress regulates MA-induced EMT.

Materials and methods

Construction of the rat model of chronic lung injury induced by MA

Twenty male Wistar rats (200 ± 10 g) from the Animal Resource Center, China Medical University (certificate number: Liaoning SCXK 2015-0001), were divided into 2 groups: control group ($n = 9$) and methamphetamine group (MA, $n = 11$). The rats in the MA group were intraperitoneally injected with MA (China Criminal Police University, China) twice a day for 6 weeks. In the 1st week, the daily dosage of MA is 10 mg/kg and then was increased by 1 mg/kg per week. At the 6th week, the daily dosage was increased to 15 mg/kg. During the time of establishing the MA model, one rat in the MA group was dead in the 3rd week, and the other in the MA group was dead in the 5th week. The rats in the control group were intraperitoneally injected with the same volume of 0.9% normal saline (Wang et al. 2018). The rats were maintained in a temperature (18–22 °C) and controlled humidity (50–70%) room and were fed with water and solid food in an alternating 12-h light and 12-h dark cycle. All the rats were weighted every day. The percentage of weight gain in each group was calculated every week using formula 1. After 6 weeks, the right ventricular index (RVI) was also calculated using formula 2 to evaluate the remodeling of the right heart resulting from chronic pulmonary dysfunction.

All animals' experimental procedures comply with the guidelines of the Guide for the Care and Use of Laboratory Animals of the National Institutes of Health (NIH), with the approval of the Institutional Animal Care and Use Committee of China Medical University (IACUC Issue No. CMU2019215).

$$\text{Percentage of the weight gain} = \frac{\text{average of the weekly weight} - \text{average of the initial weight}}{\text{average of the initial weight}} \times 100\% \quad (1)$$

$$\text{RVI} = \frac{\text{right ventricular weight}}{\text{right ventricular weight} + \text{left ventricular weight}} \times 100\% \quad (2)$$

Cell cultures and treatment

Alveolar epithelial cell lines A549 were purchased from the Beijing Dingguo Biological Technology (Beijing, China). The alveolar epithelial cells were inoculated in 6-well plates and cultured in RPMI-1640 (HyClone, USA) medium containing 10% fetal bovine serum (Clark, Australia) and 1% penicillin/streptomycin at 37 °C in 5% CO_2. A total of 1×10^5 cells in each well were cultured and then were incubated with MA at the dosage of 0.1, 0.5, 1, and 5 mM for 12, 24, and 48 h (Wang et al. 2018). To evaluate the effects of ROS scavenger, N-acetyl cysteine (NAC; N800425, Macklin, Shanghai, China), A549 cells were preincubated by 5 mM NAC (Zhou et al. 2018) dissolved in dimethyl sulfoxide (DMSO; D5879, Sigma, USA) for 1 h before 5 mM MA stimulation.

Silencing by small interfering RNA against RUNX3

The bottom of each well is covered by 70% cells. The cells were transfected with siRNA against RUNX3 (Sangon Biotech, Shanghai, China) using Lipofectamine 3000 (Thermo Fisher Scientific, USA) following the manufacturer's instructions. The following base pairs of siRNA were used for RUNX3: RUNX3-HOMO-863, (sense) 5′-CCCUGACCAUCACUGUGUUTT-3′ and (antisense) 3′-AACACAGUGAUGGUCAGGGTT-5′. After transfection for 72 h, the cells were treated with MA (5 mM, 48 h) and/or NAC (5 mM, 1 h), respectively, and were divided into the control group, the NC group, the siRUNX3 group, the

siRUNX3+NAC group, the siRUNX3+MA group, and the siRUNX3+MA+NAC group.

Hematoxylin and eosin staining

The right inferior lobes of the lungs in the control and MA groups ($n = 3$) are fixed with 4% paraformaldehyde, dehydrated, and paraffin embedded. They were sliced into 4-μm sections and stained with hematoxylin and eosin (H&E) staining. Sections on slides were placed under an optical microscope (Olympus BX 51, Japan) for observation and analysis. Chronic lung injury was evaluated by the thickness of the alveolar septum and the number of alveolar sacs (three visual fields selected randomly were analyzed in each section; magnification, × 200 and × 400) (Wang et al. 2018).

Western blotting analysis

The lung tissue ($n = 6$) and the alveolar epithelial cells were lysed in RIPA buffer with PMSF on ice and centrifuged at 14,000*g* for 15 min. Protein concentrations were measured by a BCA kit (Beyotime Biotechnology, Nanjing, China). After electrophoresis, protein was transferred to a PVDF membrane (Bio-Rad). The PVDF membrane was blocked in 5% fat-free milk for 2 h, then incubated with corresponding primary antibodies at 4 °C overnight (Table 1). The membranes were washed in Tris-buffered saline-Tween-20 (TBS-T) 3 times (10 min/time) and then incubated with horseradish peroxidase (HRP)–conjugated goat anti-rabbit or goat anti-mouse secondary antibodies (Proteintech, USA) for 2 h at room temperature, followed by detecting using enhanced chemiluminescence (ECL). The relative protein expression was quantified by densitometry using ImageQuant software (Molecular Dynamics) and normalized to β-actin. The results of RUNX3, GCS (glutamylcysteine synthetase), SOD2, E-cadherin, ZO-1, α-SMA, TGF-β1, Smad2, and p-Smad2 were represented by the relative yield to the β-actin, respectively.

Immunohistochemical assay

The 4-μm sections were processed by deparaffinization, hydration, and antigen retrieval. Primary antibodies were diluted to 1:500 and incubated with rabbit anti-ZO-1 (21773-1-AP, Proteintech, USA), anti-α-SMA (55135-1-AP, Proteintech, USA), and 1:1000 anti-RUNX3 (13089S, Cell Signaling Technology, USA) overnight at 4 °C. The sections were incubated with goat anti-rabbit biotinylated secondary antibody for 10 min at room temperature and then reacted with conjugated streptavidin-peroxidase (MXB, Fuzhou, China) for 10 min at room temperature. The sections were dipped into diaminobenzidine (DAB, Zhongshan Jinqiao, Beijing, China) and counterstained with hematoxylin and then observed under an optical microscope (Olympus BX 51, Japan).

Flow cytometry for determination of ROS

DCFH-DA can pass freely through the cell membrane and is nonfluorescent. It is hydrolyzed by the esterase in the cells to form DCFH after entering the cells. DCFH cannot penetrate the cell membrane and can be oxidized into fluorescent DCF by intracellular ROS. The fluorescence spectrum of DCF is very similar to FITC, so the fluorescence intensity of DCF can be detected by setting FITC parameters. Therefore, DCF fluorescence intensity was measured to evaluate the levels of ROS in the cells.

A549 cells (1×10^5 cells/well) were collected and seeded into 6-well plates, washed by PBS, incubated with thousand times diluted DCFH-DA (Genview, USA) with serum-free RPMI-1640 medium, and then incubated in the CO_2 incubator for 1 h at 37 °C in a dark and humidified atmosphere. The treated cells were washed with serum-free RPMI-1640 medium and collected with PBS to make a suspension. Flow cytometry was used to detect the relative fluorescence intensity of ROS.

Table 1 Primary antibodies in this study

Primary antibody	Dilution	Company	Catalog
RUNX3	1:1000	Cell Signaling Technology, USA	13089S
SOD2	1:1000	Proteintech, USA	24127-1-AP
GCS	1:1000	Proteintech, USA	12601-1-AP
E-cadherin	1:1000	Proteintech, USA	20874-1-AP
ZO-1	1:500	Proteintech, USA	21773-1-AP
α-SMA	1:500	Proteintech, USA	55135-1-AP
TGF-β1	1:500	Proteintech, USA	18978-1-AP
Smad2	1:1000	ABclonal, China	A0440
p-Smad2	1:500	Affinity Biosciences, USA	AF3449
β-actin	1:10,000	Proteintech, USA	66009-1-lg

Immunofluorescence assay

The cells were cultured in the 6-well plates and treated with MA or/and NAC. The cells were fixed in 4% paraformaldehyde and then were permeabilized in 0.2% Triton X-100 before blocking in 3% BSA for 1 h. The cells were incubated with primary antibodies: monoclonal mouse anti-ZO-1 (66452-1-lg, 1:200, Proteintech, USA) and monoclonal rabbit anti-α-SMA (55135-1-AP, 1:200, Proteintech, USA) overnight at 4 °C. The CY3-conjugated goat anti-mouse IgG and FITC-conjugated goat anti-rabbit IgG secondary antibodies (1:100, Proteintech, USA) were incubated for 1 h at room temperature in the dark. After DAPI (Beyotime Biotechnology, China) was added into each well, the mixture was incubated in the dark at room temperature for another 5 min. All the specimens were observed in × 100 oil immersion lens of a Nikon Eclipse Ni epifluorescence microscope (Nikon Instruments Inc., Tokyo, Japan).

Statistical analysis

All the data are expressed as mean ± standard deviation (SD). Statistical analysis was performed with IBM SPSS Statistics 22.0 and GraphPad Prism 6.0 (GraphPad Software, Inc., San Diego, CA, USA). Statistical comparisons were performed using the *t* test and one-way ANOVA followed by the LSD post hoc test. The values of $P < 0.05$ were considered to indicate a statistically significant difference.

Results

MA induced chronic lung injury

H&E staining was used to show the pathological changes of the lungs of rats. In the control group, the alveolar structure was intact and there was no infiltration of inflammatory cells and no thickening of the alveolar walls (Fig. 1a). But chronic exposure to MA caused more compact parenchyma, the reduction in the number of alveolar sacs, and the thickening of the alveolar walls (Fig. 1b, c). The percentage of weight gain in the MA group was significantly lower than that in the control group from 4th to 6th week (Fig. 1d). The right ventricular index (RVI) 0.19 ± 0.035 from the control group was significantly increased to 0.33 ± 0.008 in the MA group ($^{**}P < 0.01$ vs. control, Fig. 1e).

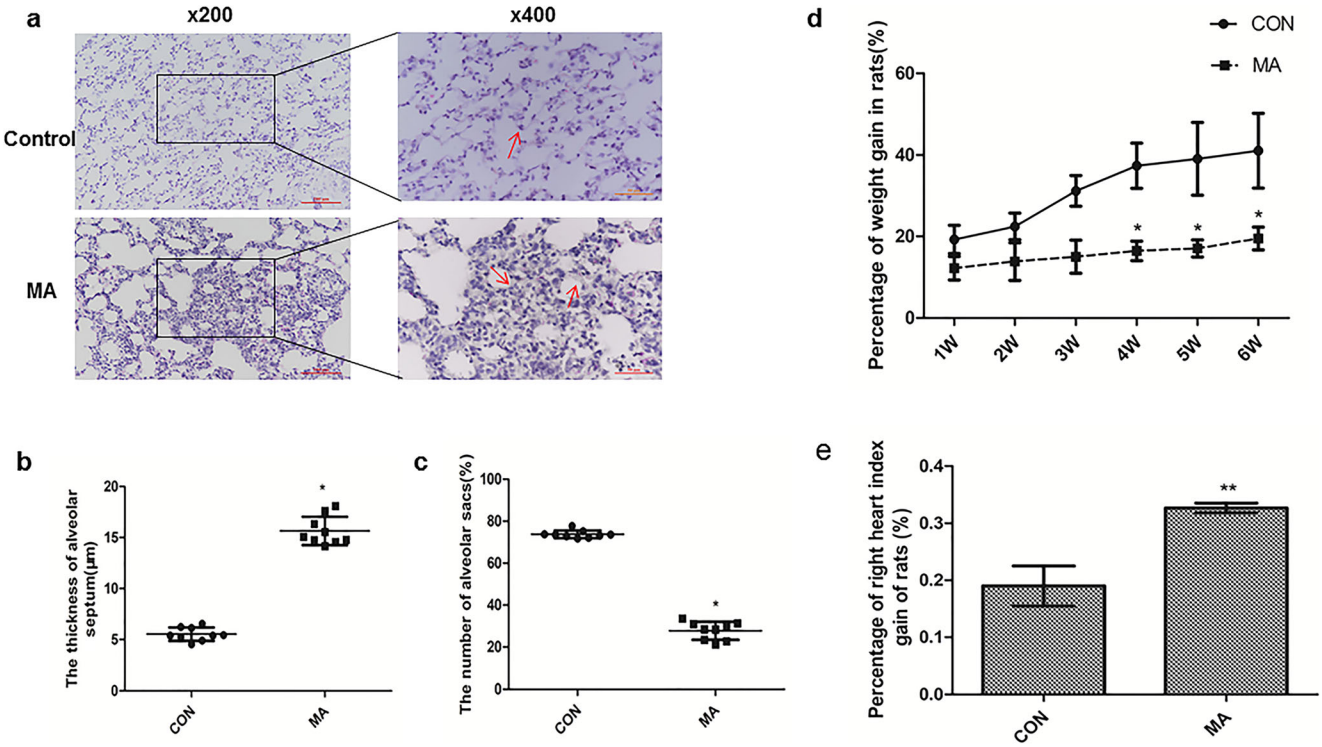

Fig. 1 MA induced chronic lung injury. **a** MA-induced chronic lung injury by H&E staining (Olympus BX 51, Japan, × 200 and × 400). Long-term exposure to MA caused more compact lung parenchyma, the thickened alveolar septum, and the reduced number of alveolar sacs. **b** The thickness of the alveolar septum. **c** The number of alveolar sacs. **d** Percentage of weight gain of rats in the Con and MA groups ($n = 9$). **e** Percentage of right heart index gain of rats in the CON and MA groups ($n = 9$). The quantification of **b** and **c** was 11analyzed in 3 visual fields randomly selected in a section ($n = 3$), respectively. Data are presented as the mean ± SD. $^{*}P < 0.05$, $^{**}P < 0.01$ vs. CON. CON, control; MA, methamphetamine

MA induced EMT in lungs and alveolar epithelial cells

Western blot analysis showed that the epithelial marker proteins E-cadherin and ZO-1 in lungs were decreased in the MA group but that there was an increase of mesenchymal marker gene α-SMA expression, compared with the control group (Fig. 2a–d). In Fig. 2i, ZO-1was expressed highly and localized at tight junctions in the control group, but in the MA group, ZO-1 expression was diminished. The expression of α-SMA in the MA group was much higher than that in the control group (Fig. 2j). When alveolar epithelial cells were treated with MA (0.1, 0.5, 1, and 5 mM) for 12, 24, and 48 h, MA reduced the levels of ZO-1 and E-cadherin and increased the levels of α-SMA at time- and dose-dependent manners compared with the control group (Fig. 2e). Specifically, there were reductions in ZO-1 and E-cadherin and upregulated expression of α-SMA by 5 mM MA at 48 h (Fig. 2f–h). The above results indicated that long-term administration with MA can cause EMT in lung tissue or alveolar epithelial cells.

The effect of MA on oxidative stress and RUNX3

Oxidative enzyme superoxide dismutase (SOD) reflects the degree of oxidative stress injury (Rodriguez-Iturbe et al. 2007; Langer 2012). Antioxidative enzyme glutamylcysteine synthetase (GCS) can scavenge oxygen free radicals (Lim et al. 2015). In our study, MA caused higher expression of SOD2 and lower expression of GCS in lungs (Fig. 3a–c). Western blot analysis showed that compared with the control group, RUNX3 in lungs was dramatically decreased in the MA group (Fig. 3a, d), which was consistent with the result from the immunohistochemistry analysis (Fig. 3e). The main cause of oxidative stress is excessive production of ROS (Kong et al. 2014; Lim et al. 2015). Flow cytometry was used to analyze the levels of ROS in living cells by measuring 1×10^5 cells and found that MA significantly augmented the production of intracellular ROS (Fig. 3f, g). RUNX3 expression in alveolar epithelial cells was inhibited by MA (Fig. 3h). Specifically, RUNX3 reduction was most prominent by 5 mM MA at 48 h (Fig. 3i).

The effect of oxidative stress on RUNX3 and EMT

To investigate if oxidative stress further affected RUNX3 and EMT, the alveolar epithelial cells were treated with the ROS scavenger NAC. MA increased SOD2 and decreased GCS, but in the NAC+MA group, the expression of SOD2 was much lower and the expression of GCS was much higher than

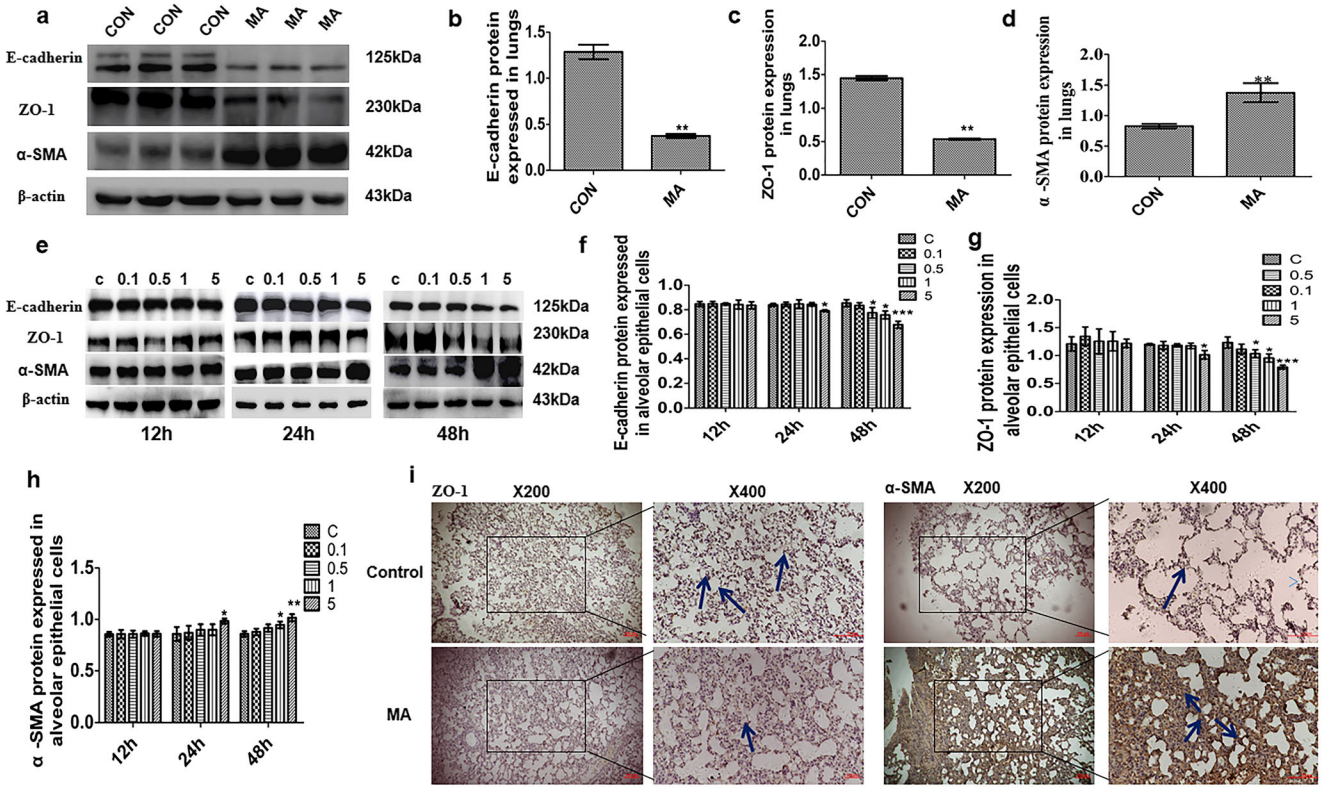

Fig. 2 MA induced EMT in lungs and alveolar epithelial cells. **a**–**d** EMT marker proteins E-cadherin, ZO-1, and α-SMA expressed in lungs by Western blot. **e**–**h** The expression of E-cadherin, ZO-1, and α-SMA in alveolar epithelial cells. **i** Expression of ZO-1 in lungs in the CON and MA groups by IHC staining. **j** Expression of α-SMA in lungs in the CON and MA groups by IHC staining. The arrows indicate the expression of ZO-1 (brown) or α-SMA (brown) in the alveolar epithelium in different groups. Data are presented as the mean ± SD. $^*P < 0.05$, $^{**}P < 0.01$ vs. CON. C, control; 0.1, 0.1 mM MA; 0.5, 0.5 mM MA; 1, 1 mM MA; 5, 5 mM MA; MA, methamphetamine

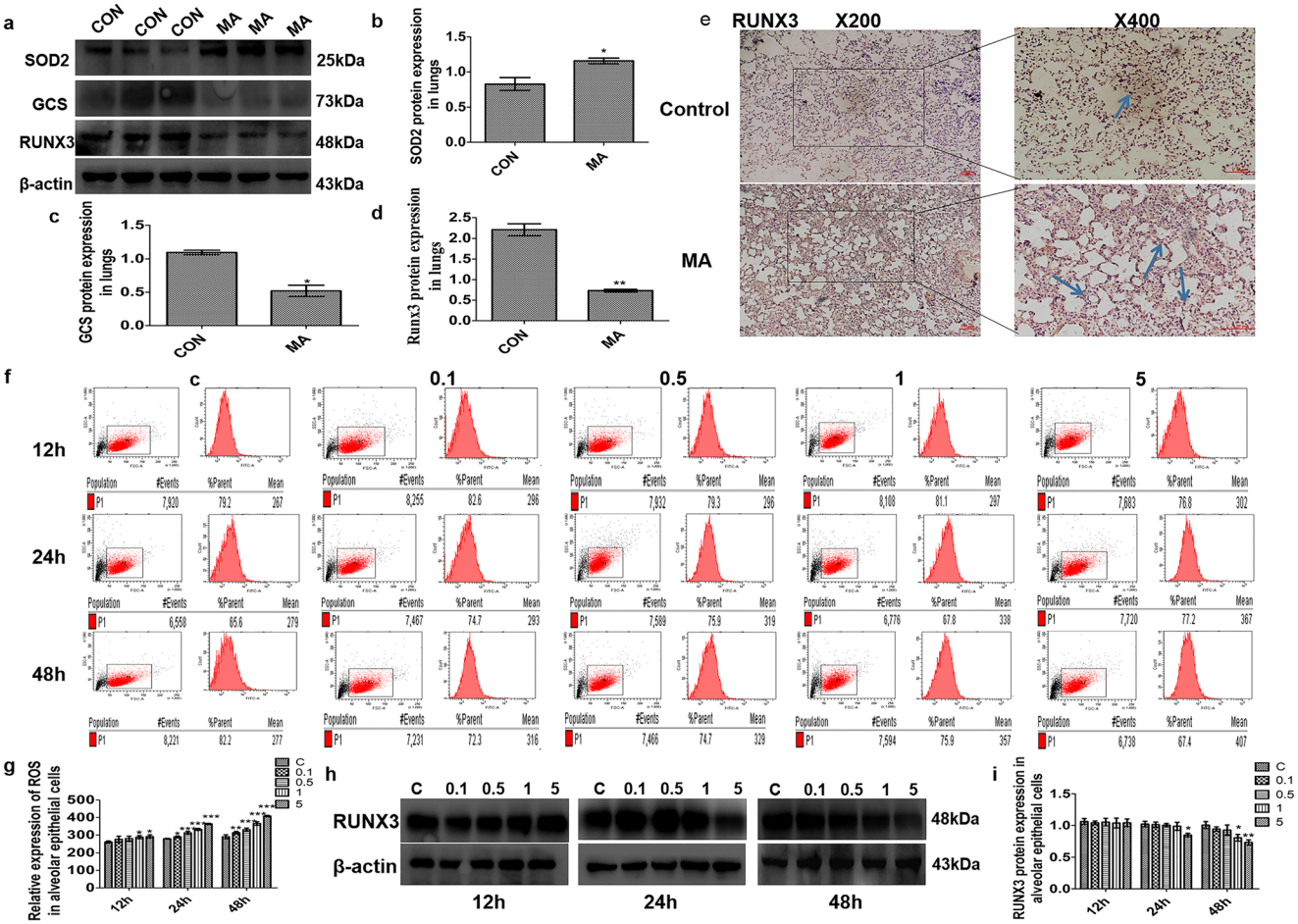

Fig. 3 The effect of MA on oxidative stress and RUNX3. **a**–**d** Effects of MA on the expression of SOD2, GCS, and RUNX3 in lungs. **e** Expression of RUNX3 in lungs in the CON and MA groups by immunohistochemical staining. The arrows indicate that sections were stained with rabbit anti-RUNX3 (brown) in the CON and MA groups. **f**, **g** ROS levels in the alveolar epithelial cells by flow cytometry. The mean value in P1 is the average fluorescence intensity, as a statistical indicator, representing the expression of ROS. **h**, **i** Expression of RUNX3 in alveolar epithelial cells. Data are presented as the mean ± SD. $^{*}P < 0.05$, $^{**}P < 0.01$, $^{***}P < 0.001$ vs. CON; C, control; 0.1, 0.1 mM MA; 0.5, 0.5 mM MA; 1, 1 mM MA; 5, 5 mM MA; MA, methamphetamine

those in the MA group (Fig. 4a–c), indicating that NAC attenuated MA-induced oxidative stress. The level of RUNX3 was significantly upregulated in the NAC+MA group in comparison with the MA group (Fig. 4d). MA caused the occurrence of EMT with the reduction in the epithelial markers E-cadherin and ZO-1 and with the increase in the mesenchymal cell marker α-SMA, which were reversed by NAC from MA (Fig. 4e–g). MA reduced the ratio of ZO-1/α-SMA that was upregulated in the NAC+MA group, compared with the MA group (Fig. 4h, i). These results suggested that pulmonary EMT by MA was associated with oxidative stress.

RUNX3-denpendent oxidative EMT induced by MA through TGF-β signaling

In order to determine the role of RUNX3 in pulmonary EMT, the siRUNX3 plasmids were transfected into the alveolar epithelial cells. After incubation for 72 h, transfected efficiency was confirmed by Western blot analysis (Fig. 5a, b). In comparison with the control group, RUNX3 was significantly decreased in the siRUNX3 group ($^{###}P < 0.001$ vs. CON), indicating that siRNA transfection is successful.

To observe the relationship between RUNX3 and oxidative stress, the alveolar epithelial cells were treated and divided into the CON group, NAC group, NC group, siRUNX3 group, and siRUNX3+NAC group. Flow cytometry analysis in Fig. 5c showed that compared with the control group, the level of ROS in the siRUNX3 and siRUNX3+NAC groups was significantly increased; compared with the siRUNX3 group, ROS production was significantly reduced in the siRUNX3+NAC group; and the ROS level in the siRUNX3+NAC group was more than that in the NAC group (Fig. 5d). These results indicate that lower RUNX3 can cause oxidative stress, so RUNX3 was closely related to oxidative stress.

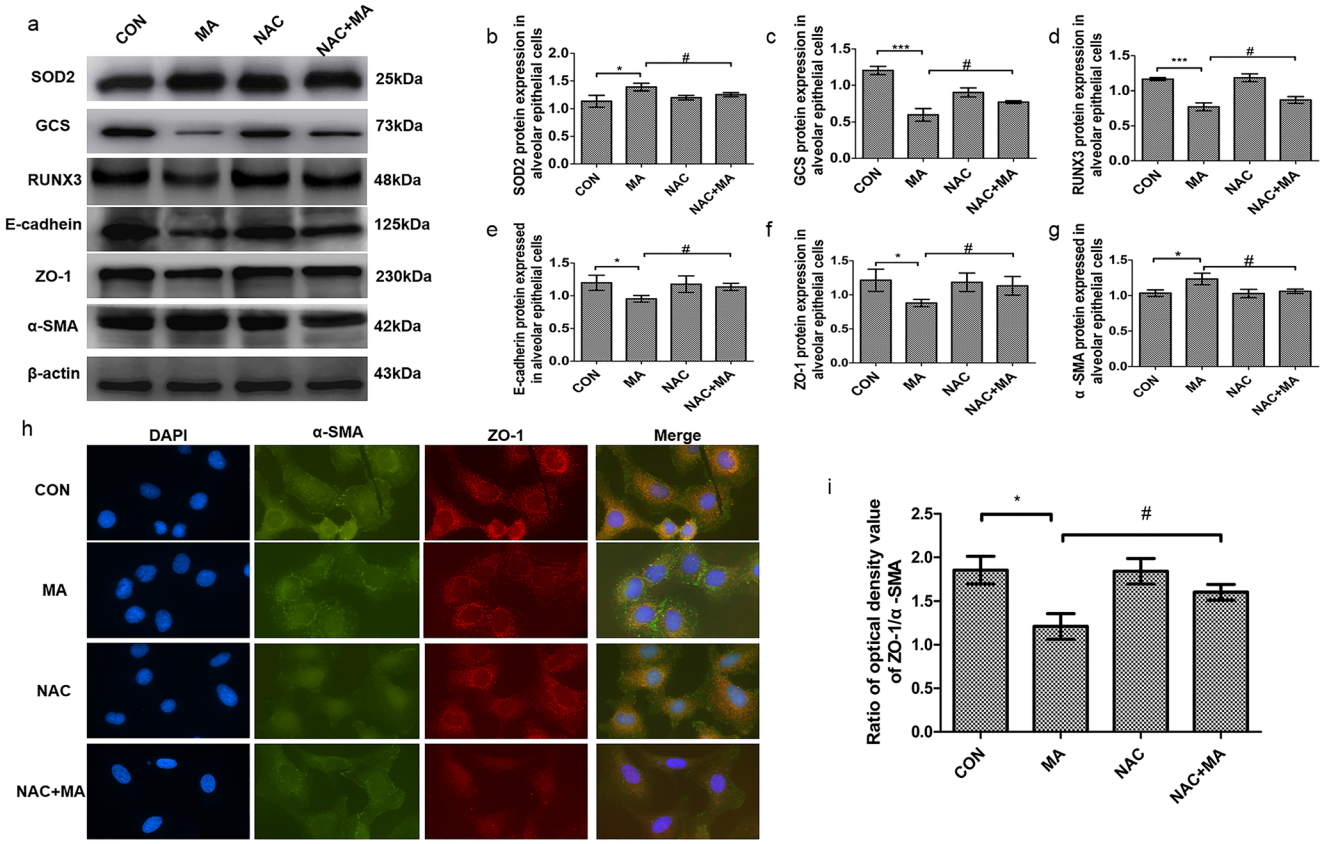

Fig. 4 The effect of oxidative stress on RUNX3 and EMT. **a** Expression of SOD2, GCS, RUNX3, E-cadherin, ZO-1, and α-SMA in the alveolar epithelial cells by Western blot. **b** SOD2 protein expression in alveolar epithelial cells. **c** GCS protein expression in alveolar epithelial cells. **d** RUNX3 protein expression in alveolar epithelial cells. **e**–**g** EMT marker proteins E-cadherin, ZO-1, and α-SMA expressed in alveolar epithelial cells. **h**, **i** Immunofluorescence assay of α-SMA and ZO-1 in alveolar epithelial cells. The cells were treated with MA (5 mM, 48 h) and/or NAC (5 mM, 1 h), respectively. Data are presented as the mean ± SD. $^{*}P < 0.05$, $^{**}P < 0.01$, $^{***}P < 0.001$ vs. CON; $^{\#}P < 0$ .05 vs. MA; NAC, N-acetyl cysteine; MA, methamphetamine

Next, the alveolar epithelial cells were separately treated and divided into the CON group, NC group, siRUNX3 group, siRUNX3+MA group, and siRUNX3+MA+NAC group. TGF-β1 and p-Smad2 were significantly increased in the siRUNX3, siRUNX3+MA, and siRUNX3+MA+NAC groups (Fig. 5e–g, $P < 0.05$, $P < 0.001$ vs. CON). After knockdown of RUNX3, the levels of TGF-β1 and p-Smad2 were further upregulated by MA but were reversed by NAC from MA (Fig. 5e–g). And then, in Fig. 5h, E-cadherin and ZO-1 were reduced and α-SMA was increased in the siRUNX3 group and in the siRUNX3+MA group. Compared with the siRUNX3+MA group, E-cadherin and ZO-1 were significantly increased and the expression of α-SMA was decreased in the siRUNX3+MA+NAC group (Fig. 5i–k). Immunofluorescence assay results of α-SMA and ZO-1 were consistent with Western blot (Fig. 5l, m). These results suggest that RUNX3 is the key to oxidative EMT induced by MA and that RUNX3-denpendent anti-oxidative stress can alleviate MA-induced EMT through TGF-β signaling.

Discussion

Chronic exposure to MA resulted in the lower growth ratio of weight, increased RVI, and chronic lung injury including the thickened alveolar walls and the reduced number of alveolar sacs. Long-term administration with MA caused oxidative stress and reduced the expression of RUNX3 in alveolar epithelial cells. NAC alleviated pulmonary EMT, suggesting that EMT by MA was associated with oxidative stress. After knockdown of RUNX3, ROS levels were significantly upregulated, indicating that RUNX3 was closely related to oxidative stress. siRUNX3 made MA further decrease E-cadherin and ZO-1 and increase α-SMA by activating RUNX3-dependent TGF-β signaling. But the aggravated EMT was significantly reversed by the inhibition of RUNX3-related oxidative stress. These results indicate that long-term exposure to MA can induce pulmonary EMT, that pulmonary EMT was associated with oxidative stress, that RUNX3 was the key to oxidative EMT induced by MA, and that the inhibition of RUNX3-related oxidative stress can alleviated MA-induced EMT through TGF-β signaling.

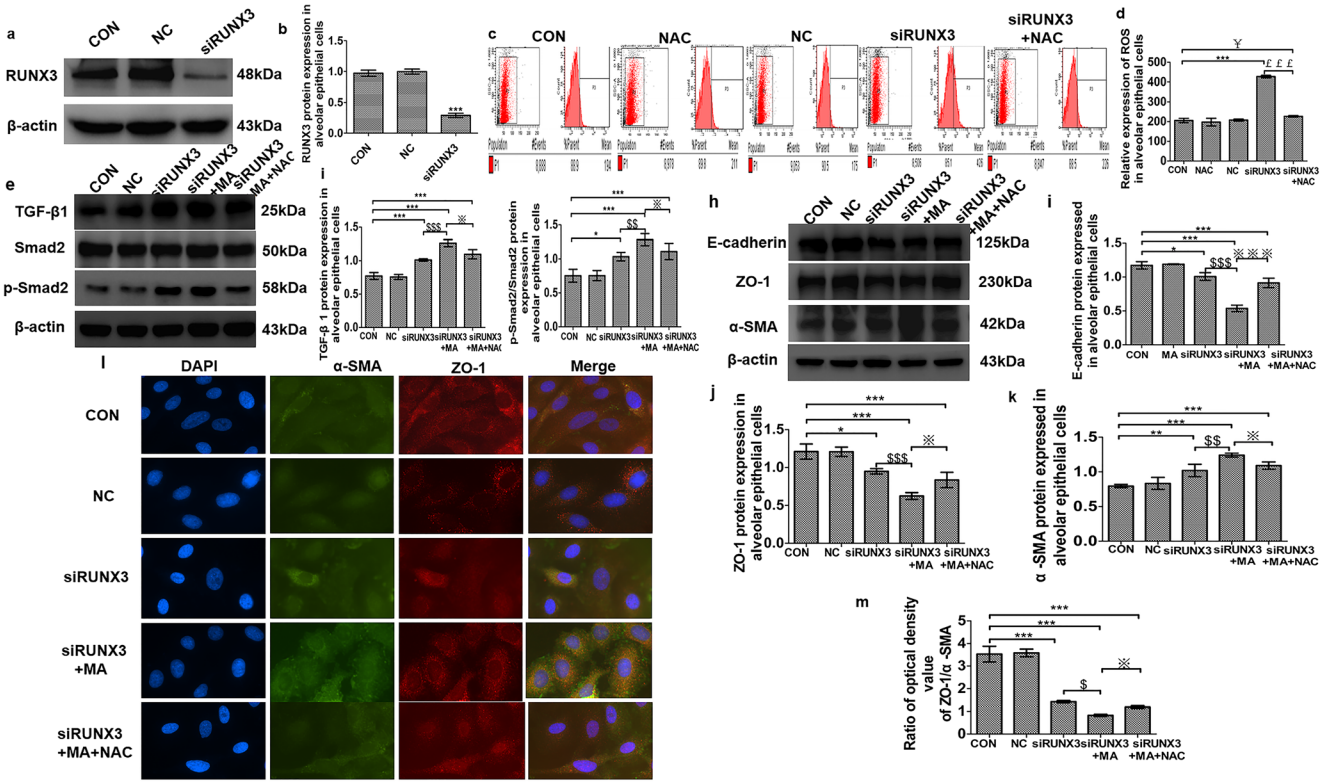

Fig. 5 RUNX3-related oxidative EMT induced by MA through TGF-β signaling. **a**, **b** The expression of RUNX3 after transfection by Western blot assay. **c**, **d** ROS levels in the alveolar epithelial cells by flow cytometry. The mean value in P1 is the average fluorescence intensity, as a statistical indicator, representing the expression of ROS. (**e**) TGF-β signaling expression by Western blot. **f** TGF-β 1 expression in alveolar epithelial cells in the various groups. **g** p-Smad2/Smad2 expression in alveolar epithelial cells in the various groups. **h**–**k** EMT marker proteins E-cadherin, ZO-1, and α-SMA expressed in alveolar epithelial cells in the various groups. **l**, **m** Immunofluorescence assay of α-SMA and ZO-1 in alveolar epithelial cells. After transfection for 72 h, the cells were treated with MA (5 mM, 48 h) and/or NAC (5 mM, 1 h), respectively. Data are presented as the mean ± SD. $^{*}P < 0.05$, $^{**}P < 0.01$, $^{***}P < 0.001$ vs. CON group; $^{\#}P < 0.05$ vs. NAC; $^{\$}P < 0.05$, $^{\$\$}P < 0.01$, $^{\$\$\$}P < 0.001$ vs. siRUNX3; $P < 0.05$, $P < 0.001$ vs. siRUNX3+MA. CON, control; NC, negative control (empty plasmid); siRUNX3, siRNA against RUNX3; NAC, N-acetyl cysteine; MA, methamphetamine

The high uptake and accumulation of MA in the lungs resulted in chronic lung injury (Park et al. 2012). In the present study, pulmonary toxicity was prominent under the exposure to MA from 4th to 6th week. MA caused the slower growth ratio of weight and even individual death. Morphological results showed that the alveolar walls were thickened, that pulmonary alveoli were fused, and that the number of alveolar sacs was reduced. These suggested that long-term exposure to MA induced chronic lung injury in rats.

EMT plays an important role in various physiological processes, especially in lung development and some lung diseases, such as pulmonary fibrosis, chronic obstructive pulmonary disease (COPD), and lung cancer (Stone et al. 2016). EMT is defined as the process by which phenotypic changes fix in the epithelial cells, manifesting that the epithelial cells lose the epithelial marker protein such as E-cadherin responsible for tight junctions (Karicheva et al. 2016) and then convert into the mesenchymal phenotype after acquiring the mesenchymal markers such as α-SMA (Lu et al. 2017). The results from our study show that MA significantly decreased epithelial marker proteins E-cadherin and ZO-1 but significantly increased the expression of the mesenchymal marker gene α-SMA in lungs and in alveolar epithelial cells. These changes were in accordance with other drug-induced EMT (Chen et al. 2016; Yang et al. 2018), reflecting that pulmonary EMT could be induced by the long-term administration with MA. In addition, ROS scavenger NAC significantly reversed the expression of E-cadherin, ZO-1, and α-SMA and upregulated the ratio of ZO-1/α-SMA from MA. These results suggest that pulmonary EMT by MA was associated with oxidative stress.

RUNX3 acts as the smallest member of the RUNX family to inhibit tumor formation. Although most research studies about RUNX3 have focused on cancer (Xu et al. 2012; Lotem et al. 2015; Gou et al. 2017; Chen et al. 2019), RUNX3 also plays a key role in cell growth, vascular development, and immune regulation (Lee et al. 2010, 2014; Lotem et al., 2017). Interestingly, there is a crosstalk between RUNX3 and oxidative stress (Kang et al. 2013; Poungpairoj et al. 2015). Oxidative stress is an imbalance between the production of ROS and the detoxification capabilities (Kang et al. 2017). In the present research, long-term exposure to

MA not only significantly decreased the expression of RUNX3 in vivo and vitro but also increased ROS levels and caused redox imbalance by reducing GCS and increasing SOD. To investigate if RUNX3 is related to oxidative stress–induced by MA, the alveolar epithelial cells were transfected with siRUNX3 or/and treated with the ROS scavenger NAC. Our study shows that compared with the control group, the level of ROS in the siRUNX3 and siRUNX3+NAC groups was significantly increased; compared with the siRUNX3 group, ROS production was significantly reduced in the siRUNX3+NAC group; in addition, the ROS level in the siRUNX3+NAC group was more than that in the NAC group. These results indicate that lower RUNX3 can cause oxidative stress, so RUNX3 is closely related to oxidative stress.

The occurrence of EMT is affected by some mechanisms including the TGF-β signaling pathway, Wnt signaling pathway, and Notch signaling pathway (Savagner 2001; Wang et al. 2019; Xiang et al. 2019). TGF-β is one of the most important inducers for EMT involved in organ fibrosis, embryo development, and tumor metastasis (Dong et al. 2017). RUNX3 is a key regulator of the TGF-β signaling pathway by interacting with R-Smads (Krishnan and Ito 2017). The increased proliferation and suppressed apoptosis of gastric epithelial cells with RUNX3$^{-/-}$ were attributed to defective TGF-β signaling (Voon et al. 2012). In our present study, TGF-β1 and p-Smad2 were significantly increased in the siRUNX3, siRUNX3+MA, and siRUNX3+MA+NAC groups. After knockdown of RUNX3, the levels of TGF-β1 and p-Smad2 were further upregulated by MA but were reversed by NAC from MA. E-cadherin and ZO-1 were reduced, and α-SMA was increased in the siRUNX3 group and in the siRUNX3+MA group. Compared with the siRUNX3+MA group, E-cadherin and ZO-1 were significantly increased and the expression of α-SMA was significantly decreased in the siRUNX3+MA+NAC group. Immunofluorescence assay results of α-SMA and ZO-1 were consistent with Western blot. In a follow-up work, we will use the technique of Cre-loxP Knockout in rats to further confirm the relationship among RUNX3, oxidative stress, and EMT induced by MA. But these present results suggest that RUNX3 is related to oxidative EMT induced by MA and that the inhibition of RUNX3-dependent oxidative stress can alleviate MA-induced EMT through TGF-β signaling.

In summary, RUNX3 may be the key to oxidative EMT in methamphetamine-induced chronic lung injury.

Funding information This research was funded by the National Natural Science Foundation of China (Nos. 81973404 and 81503058), Department of Education of Liaoning Province (No. JC2019034), and Natural Science Foundation of Liaoning Province (No. 2014021065).

Data availability The data that support the findings of this study are available from the corresponding author upon reasonable request.

Compliance with ethical standards

All animals' experimental procedures comply with the guidelines of the Guide for the Care and Use of Laboratory Animals of the National Institutes of Health (NIH), with the approval of the Institutional Animal Care and Use Committee of China Medical University (IACUC Issue No. CMU2019215).

Competing interests The authors declare that they have no competing interests.

References

Albertson TE, Derlet RW, Van Hoozen BE (1999) Methamphetamine and the expanding complications of amphetamines. West J Med Apr 170(4):214–219

Bai Y, Wang Y, Liu M, Gu YH, Jiang B, Wu X, Wang HL (2017) Suppression of nuclear factor erythroid-2-related factor 2-mediated antioxidative defense in the lung injury induced by chronic exposure to methamphetamine in rats. Mol Med Rep 15(5):3135–3142

Chen F, Liu X, Cheng Q, Zhu S, Bai J, Zheng J (2017) RUNX3 regulates renal cell carcinoma metastasis via targeting miR-6780a-5p/E-cadherin/EMT signaling axis. Oncotarget 8(60):101042–101056

Chen K, Liu H, Liu Z, Luo S, Patz EF, Moorman PG, Su L, Shen S, Christiani DC, Wei Q (2019) Genetic variants in RUNX3, AMD1 and MSRA in the methionine metabolic pathway and survival in nonsmall cell lung cancer patients. Int J Cancer 145(3):621–631

Chen KJ, Li Q, Wen CM, Duan ZX, Zhang JY, Xu C, Wang JM (2016) Bleomycin (BLM) induces epithelial-to-mesenchymal transition in cultured A549 cells via the TGF-β/Smad signaling pathway. J Cancer 7(11):1557–1564

Choi SS, Diehl AM (2009) Epithelial-to-mesenchymal transitions in the liver. Hepatology 50(6):2007–2013

Ciccarone D (2011) Stimulant abuse: pharmacology, cocaine, methamphetamine, treatment, attempts at pharmacotherapy. Prim Care 38(1):41–58

Dong N, Shi L, Wang DC, Chen C, Wang X (2017) Role of epigenetics in lung cancer heterogeneity and clinical implication. Semin Cell Dev Biol 64:18–25

Franco R, Schoneveld O, Georgakilas AG, Panayiotidis MI (2008) Oxidative stress, DNA methylation and carcinogenesis. Cancer Lett 266(1):6–11

Gou Y, Zhai F, Zhang L, Cui L (2017) RUNX3 regulates hepatocellular carcinoma cell metastasis via targeting miR-186/E-cadherin/EMT pathway. Oncotarget 8(37):61475–61486

Ito Y, Bae SC, Chuang LS (2015) The RUNX family: developmental regulators in cancer. Nat Rev Cancer 15(2):81–95

Jolly MK, Ward C, Eapen MS (2018) Epithelial-mesenchymal transition, a spectrum of states: role in lung development, homeostasis, and disease. Dev Dyn 247(3):346–358

Kang KA, Kim KC, Bae SC, Hyun JW (2013) Oxidative stress induces proliferation of colorectal cancer cells by inhibiting RUNX3 and activating the Akt signaling pathway. Int J Oncol 43(5):1511–1516

Kang KA, Piao MJ, Ryu YS, Maeng YH, Hyun JW (2017) Cytoplasmic localization of RUNX3 via histone deacetylase-mediated SRC expression in oxidative-stressed colon cancer cells. J Cell Physiol 232(7):1914–1921

Karicheva O, Rodriguez-Vargas JM, Wadier N, Martin-Hernandez K, Vauchelles R, Magroun N, Tissier A, Schreiber V, Dantzer F (2016) PARP3 controls TGFβ and ROS driven epithelial-to-mesenchymal transition and stemness by stimulating a TG2-Snail-E-cadherin axis. Oncotarget 7(39):64109–64123

Komori T (2017) Roles of Runx2 in skeletal development. Adv Exp Med Biol 962:83–93

Kong Y, Trabucco SE, Zhang H (2014) Oxidative stress, mitochondrial dysfunction and the mitochondria theory of aging. Interdiscip Top Gerontol 39:86–107

Krishnan V, Ito Y (2017) RUNX3 loss turns on the dark side of TGF-beta signaling. Oncoscience 4(11–12):156–157

Kulkarni M, Tan TZ, Syed SNB, Lamar JM, Bansal P, Cui J, Qiao Y, Ito Y (2018) RUNX1 and RUNX3 protect against YAP-mediated EMT, stem-ness and shorter survival outcomes in breast cancer. Oncotarget 9(18):14175–14192

Langer M (2012) Bacillus anthracis lethal toxin reduces human alveolar epithelial barrier function. 80(12):4374–4387

Lee JM, Kwon HJ, Lai WF, Jung HS (2014) Requirement of Runx3 in pulmonary vasculogenesis. Cell Tissue Res 356(2):445–449

Lee KS, Lee YS, Lee JM, Ito K, Cinghu S, Kim JH, Jang JW, Li YH, Goh YM, Chi XZ, Wee H, Lee HW, Hosoya A, Chung JH, Jang JJ, Kundu JK, Surh YJ, Kim WJ, Ito Y, Jung HS, Bae SC (2010) Runx3 is required for the differentiation of lung epithelial cells and suppression of lung cancer. Oncogene 29(23):3349–3361

Lim J, Nakamura BN, Mohar I, Kavanagh TJ, Luderer U (2015) Glutamate cysteine ligase modifier subunit (Gclm) null mice have increased ovarian oxidative stress and accelerated age-related ovarian failure. Endocrinology 156(9):3329–3343

Link KA, Chou FS, Mulloy JC (2010) Core binding factor at the crossroads: determining the fate of the HSC. J Cell Physiol 222(1):50–56

Lotem J, Levanon D, Negreanu V, Bauer O, Hantisteanu S, Dicken J, Groner Y (2015) Runx3 at the interface of immunity, inflammation and cancer. Biochim Biophys Acta 1855(2):131–143

Lotem J, Levanon D, Negreanu V, Bauer O, Hantisteanu S, Dicken J, Groner Y (2017) Runx3 in immunity, inflammation and cancer. Adv Exp Med Biol 962:369–393

Lu J, Zhong Y, Lin Z, Lin X, Chen Z, Wu X, Wang N, Zhang H, Huang S, Zhu Y, Wang Y, Lin S (2017) Baicalin alleviates radiation-induced epithelial-mesenchymal transition of primary type II alveolar epithelial cells via TGF-β and ERK/GSK3β signaling pathways. Biomed Pharmacother 95:1219–1224

Orcholski ME, Khurshudyan A, Shamskhou EA, Yuan K, Chen IY, Kodani SD, Morisseau C, Hammock BD, Hong EM, Alexandrova L, Alastalo TP, Berry G, Zamanian RT, de Jesus Perez VA (2017) Reduced carboxylesterase 1 is associated with endothelial injury in methamphetamine-induced pulmonary arterial hypertension. Am J Physiol Lung Cell Mol Physiol 313(2):L252–L266

Park M, Hennig B, Toborek M (2012) Methamphetamine alters occludin expression via NADPH oxidase-induced oxidative insult and intact caveolae. J Cell Mol Med 16(2):362–375

Poungpairoj P, Whongsiri P, Suwannasin S, Khlaiphuengsin A, Tangkijvanich P, Boonla C (2015) Increased oxidative stress and RUNX3 hypermethylation in patients with hepatitis B virus-associated hepatocellular carcinoma (HCC) and induction of RUNX3 hypermethylation by reactive oxygen species in HCC cells. Asian Pac J Cancer Prev 16(13):5343–5348

Ramirez RL, Perez VJ, Zamanian RT (2018) Methamphetamine and the risk of pulmonary arterial hypertension. Curr Opin Pulm Med 24(5): 416–424

Rodriguez-Iturbe B, Sepassi L, Quiroz Y, Ni Z, Wallace DC, Vaziri ND (2007) Association of mitochondrial SOD deficiency with salt-sensitive hypertension and accelerated renal senescence. J Appl Physiol (1985) 102(1): 255–260

Savagner P (2001) Leaving the neighborhood: molecular mechanisms involved during epithelial-mesenchymal transition. Bioessays 23(10):912–923

Sood R, Kamikubo Y, Liu P (2017) Role of RUNX1 in hematological malignancies. Blood 129(15):2070–2082

Stone RC, Pastar I, Ojeh N, Chen V, Liu S, Garzon KI, Tomic-Canic M (2016) Epithelial-mesenchymal transition in tissue repair and fibrosis. Cell Tissue Res 365(3):495–506

Volkow ND, Fowler JS, Wang GJ, Shumay E, Telang F, Thanos PK, Alexoff D (2010) Distribution and pharmacokinetics of methamphetamine in the human body: clinical implications. PLoS One 5(12):e15269

Voon DC, Wang H, Koo JK, Nguyen TA, Hor YT, Chu YS, Ito K, Fukamachi H, Chan SL, Thiery JP, Ito Y (2012) Runx3 protects gastric epithelial cells against epithelial-mesenchymal transition-induced cellular plasticity and tumorigenicity. Stem Cells 30(10): 2088–2099

Wang Y, Gu YH, Liang LY, Liu M, Jiang B, Zhu MJ, Wang X, Shi L (2018) Concurrence of autophagy with apoptosis in alveolar epithelial cells contributes to chronic pulmonary toxicity induced by methamphetamine. Cell Prolif 51(5):e12476

Wang DP, Tang XZ, Liang QK, Zeng XJ, Yang JB, Xu J (2019) microRNA-599 promotes apoptosis and represses proliferation and epithelial-mesenchymal transition of papillary thyroid carcinoma cells via downregulation of Hey2-depentent Notch signaling pathway. J Cell Physiol

Whittle MC, Hingorani SR (2015) Disconnect between EMT and metastasis in pancreas cancer. Oncotarget 6(31):30445–30446

Xiang X, Xiong R, Yu C, Deng L, Bie J, Xiao D, Chen Z, Zhou Y, Li X, Liu K, Feng G (2019) Tex10 promotes stemness and EMT phenotypes in esophageal squamous cell carcinoma via the Wnt/β-catenin pathway. Oncol Rep

Xu N, Shen C, Luo Y, Xia L, Xue F, Xia Q, Zhang J (2012) Upregulated miR-130a increases drug resistance by regulating RUNX3 and Wnt signaling in cisplatin-treated HCC cell. Biochem Biophys Res Commun 425(2):468–472

Yang L, Jiao X, Wu J, Zhao J, Liu T, Xu J, Ma X, Cao L, Liu L, Liu Y, Chi J, Zou M, Li S, Xu J, Dong L (2018) Cordyceps sinensis inhibits airway remodeling in rats with chronic obstructive pulmonary disease. Exp Ther Med 15(3):2731–2738

Zhou J, An X, Dong J, Wang Y, Zhong H, Duan L, Ling J, Ping F, Shang J (2018) IL-17 induces cellular stress microenvironment of melanocytes to promote autophagic cell apoptosis in vitiligo. FASEB J 32(9):4899–4916